nature immunology

Macrophage colony-stimulating factor induces the proliferation and survival of macrophages via a pathway involving DAP12 and β-catenin

Karel Otero[1], Isaiah R Turnbull[1], Pietro Luigi Poliani[2], William Vermi[2], Elisa Cerutti[1], Taiki Aoshi[1,5], Ilaria Tassi[1], Toshiyuki Takai[3], Samuel L Stanley[4], Mark Miller[1], Andrey S Shaw[1] & Marco Colonna[1]

Macrophage colony-stimulating factor (M-CSF) influences the proliferation and survival of mononuclear phagocytes through the receptor CSF-1R. The adaptor protein DAP12 is critical for the function of mononuclear phagocytes. DAP12-mutant mice and humans have defects in osteoclasts and microglia, as well as brain and bone abnormalities. Here we show DAP12 deficiency impaired the M-CSF-induced proliferation and survival of macrophages *in vitro*. DAP12-deficient mice had fewer microglia in defined central nervous system areas, and DAP12-deficient progenitors regenerated myeloid cells inefficiently after bone marrow transplantation. Signaling by M-CSF through CSF-1R induced the stabilization and nuclear translocation of β-catenin, which activated genes involved in the cell cycle. DAP12 was essential for phosphorylation and nuclear accumulation of β-catenin. Our results provide a mechanistic explanation for the many defects of DAP12-deficient mononuclear phagocytes.

Macrophage colony-stimulating factor (M-CSF (A001489); also known as colony-stimulating factor 1 (CSF-1), is the main regulator of the proliferation, survival and differentiation of mononuclear phagocytes, which include monocytes, macrophages and bone-resorbing osteoclasts and their precursors[1–3]. M-CSF acts through the receptor CSF-1R (A000674), a tyrosine kinase encoded by the proto-oncogene *Csf1r*[4] that is expressed exclusively on mononuclear phagocytes. Binding of M-CSF to CSF-1R results in the formation of receptor dimers, the autophosphorylation of several tyrosine residues located in the cytoplasmic domain and the phosphorylation of many other proteins, including the phosphatase SHP-1 and the kinases Src, PLC-γ, PI(3)K, Akt and Erk[5–8]. The M-CSF–CSF-1R complex is subsequently internalized and degraded in lysosomes. Signaling through CSF-1R is required for entry of cells into S phase[9,10] and for cell survival[11]. The biological importance of the M-CSF–CSF-1R axis is demonstrated by osteopetrotic (*op/op*) mice, which lack a functional gene encoding M-CSF (*Csf1*)[12]. These mice develop osteopetrosis due to impaired osteoclast formation, as well as deficits in blood monocytes and tissue macrophages. *In vitro*, M-CSF–CSF-1R signaling drives the proliferation and differentiation of precursor cells into macrophages or osteoclasts and is required for the survival of these cells. However, mononuclear phagocytes are not uniformly dependent on M-CSF[13]; although some subpopulations continuously require M-CSF, others, such as microglia, depend on M-CSF only in specific areas of the central nervous system (CNS)[14–16].

DAP12 (A000750) is an adaptor protein associated with several myeloid and lymphocyte receptors; these receptors require DAP12 for cell surface expression and signaling[17]. DAP12 consists of a short extracellular and transmembrane region followed by a cytoplasmic domain that contains an immunoreceptor tyrosine-based activation motif (ITAM). After engagement of the associated receptor, the DAP12 ITAM is phosphorylated and acts as a docking site for the protein tyrosine kinases Syk and Zap70, which recruit and activate multiple 'downstream' adaptors and signaling enzymes that induce cell activation. The crucial function of DAP12 and DAP12-associated receptors in the function of mononuclear phagocytes is manifested in the human disorder of Nasu-Hakola disease (NHD), which is caused by a recessive mutation in the gene encoding DAP12 or the gene encoding the associated cell surface receptor TREM-2 (refs. 18,19). NHD is characterized by brain demyelination and gliosis, which engender presenile dementia, as well as by polycystic osteodysplasia, which causes spontaneous fractures. DAP12 is expressed in microglia and osteoclasts, which suggests that NHD may result from impaired function and/or differentiation of these cells.

Three independent lines of DAP12-deficient mice have been generated, and studies of these mice have collectively confirmed the function of DAP12 in mononuclear phagocytes. DAP12-deficient mice develop osteopetrosis[20–22] because DAP12-deficient osteoclast precursors differentiate poorly into osteoclasts[20–24], mainly because of impaired integrin signaling[25]. However, whether microglia are

[1]Department of Pathology and Immunology, Washington University School of Medicine, St. Louis, Missouri, USA. [2]Department of Pathology, University of Brescia, Spedali Civili, Brescia, Italy. [3]Department of Experimental Immunology, Japan Science and Technology Agency, Tohoku University, Aoba-ku, Sendai-shi, Japan. [4]Division of Infectious Diseases, Department of Medicine, Washington University School of Medicine, St. Louis, Missouri, USA. [5]Present address: Research Institute for Microbial Diseases, Osaka University, 3-1 Yamada-oka, Suita, Osaka, Japan. Correspondence should be addressed to M.C. (mcolonna@pathology.wustl.edu).

Received 2 September 2008; accepted 22 April 2009; published online 7 June 2009; doi:10.1038/ni.1744

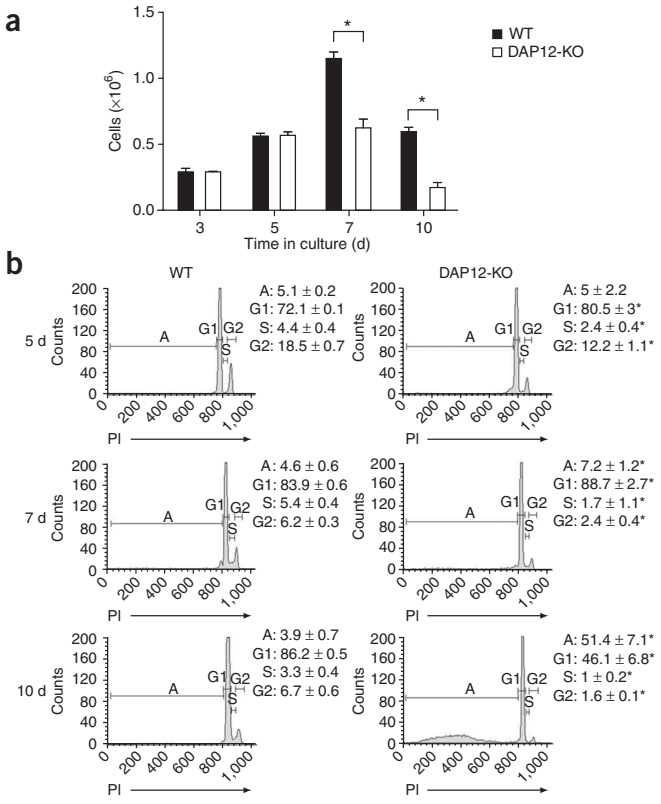

Figure 1 Lower yield of DAP12-deficient BMDM cultures. (**a**) BMDM numbers at various times (horizontal axis) of culture of wild-type (WT) and DAP12-deficient (DAP12-KO) bone marrow cells with M-CSF (mean and s.d.). $*P < 0.01$ (Student's *t*-test). (**b**) Propidium iodide (PI) analysis of the cell cycle and apoptosis of BMDM cultures at days 5, 7 and 10, with gating on apoptotic cells (A; cells with <2N DNA) and cells in the G1, S and G2 phases of the cell cycle; right margin, percentage of total cells in each gate (± s.d.). $*P < 0.05$, compared with wild-type at the same day of culture (Student's *t*-test). Data are representative of three separate experiments with two wild-type and two DAP12-deficient cultures in each.

defective in DAP12-deficient mice is unclear. One study of mice expressing a mutant DAP12 lacking its ITAM reported delayed postnatal differentiation and migration of microglia into the CNS, whereas microglia in adult mice seemed normal[22]. In contrast, a study of DAP12-deficient mice reported no defect in microglia but reported abnormal development of oligodendrocytes, hypomyelination and synaptic degeneration[20]. In addition to producing defects in osteoclasts and microglia, DAP12 deficiency also augments cytokine secretion and Erk activation in macrophages in response to microbial stimuli[26]. However, a mechanism involving DAP12 that would account for the CNS defect and the skewed macrophage activation has yet to be defined.

Here we demonstrate that DAP12-deficient mononuclear phagocytes were less responsive to M-CSF *in vitro*; as a result, DAP12-deficient phagocytic monocytes had diminished proliferation and survival. *In vivo*, DAP12 deficiency resulted in profoundly fewer microglial cells in certain areas of the CNS of older mice, as well as less regeneration of myeloid cells after bone marrow transplantation. Mechanistically, we show that CSF1-R signaling involved the stabilization, tyrosine phosphorylation and nuclear translocation of β-catenin (A000506), which are essential for the subsequent activation of genes that facilitate cell division. Notably, DAP12 was essential for optimal phosphorylation and nuclear accumulation of β-catenin. Moreover, this process involved the tyrosine kinase Pyk2 (A001952; also called CADTK). Skewed M-CSF signaling and defective proliferation and survival of DAP12-deficient mononuclear phagocytes may therefore contribute to the pathology of patients with NHD.

RESULTS

Impaired growth of DAP12-deficient macrophages

During routine culture of wild-type and DAP12-deficient bone marrow cells with M-CSF to generate bone marrow–derived macrophages (BMDMs), we noted a deficit in the yield of DAP12-deficient macrophages compared with that of wild-type macrophages. To quantify this deficiency, we cultured DAP12-deficient and wild-type bone marrow cells for 10 d with M-CSF and counted all viable cells at various time points. In wild-type cultures, the number of BMDMs increased until day 7 of culture and decreased at day 10 (**Fig. 1a**). As macrophages rapidly degrade M-CSF, this decrease may have reflected consumption of M-CSF in the cultures, which results in growth arrest and apoptosis. Notably, at day 7 and day 10, DAP12-deficient cultures had significantly fewer cells than did wild-type cultures (**Fig. 1a**).

That decrease could have been due to less proliferation or more cell death. To assess the contribution of each of these mechanisms, we collected cells at days 5, 7 and 10 of culture and analyzed cell cycle and cell death by measuring DNA content with propidium iodide. In contrast to wild-type BMDMs, DAP12-deficient BMDMs showed arrest of cells in G1 at days 5 and 7, and their cultures contained slightly more hypodiploid cells that corresponded to apoptotic cells (**Fig. 1b**). These data suggest that DAP12-deficient cells divide less efficiently than do wild-type cells in response to M-CSF at these time points. In addition, we found many more hypodiploid cells in DAP12-deficient cultures but not wild-type cultures at day 10 (**Fig. 1b**). Thus, DAP12 may be required for both M-CSF-dependent macrophage proliferation and survival, and its contribution to each process may vary at different culture stages.

DAP12 is needed for M-CSF-induced proliferation

To directly measure the effect of DAP12 deficiency on M-CSF-induced proliferation, we stimulated wild-type and DAP12-deficient BMDMs at day 5 of culture with two different concentrations of M-CSF and analyzed the cell cycle by propidium iodide staining. The percentage of DAP12-deficient BMDMs in either S or G2 phase was lower and the percentage in G1 phase was higher relative to wild-type BMDMs at each M-CSF concentration (**Fig. 2a**). Retroviral transduction of DAP12 into DAP12-deficient BMDMs reconstituted a cell cycle profile similar to that of wild-type cells (**Fig. 2b**), which directly linked DAP12 deficiency to less proliferation. We also quantified the proliferation of wild-type and DAP12-deficient BMDMs by analyzing incorporation of the thymidine analog BrdU by flow cytometry. Only 14.6% ± 1.8% of DAP12-deficient cells incorporated BrdU, compared with 44.6% ± 2.9% of wild-type cells (**Fig. 2c**), which further demonstrated a defect in the proliferative response to M-CSF in DAP12-deficient cells. To confirm the defect in cell cycling, we measured expression of mRNA transcripts encoding cell cycle–regulatory proteins in BMDMs. Compared with wild-type cells, DAP12-deficient cells expressed less c-Myb mRNA at day 5 and less c-Myc, cyclin D1 and cyclin D2 mRNA at days 5 and 7 of culture (**Fig. 2d**). To rule out the possibility that DAP12-deficient BMDMs proliferate poorly in response to M-CSF because of a general defect in macrophage differentiation, we transduced wild-type BMDMs with retrovirus encoding a dominant negative form of DAP12

(DAP12-DN) that lacks a functional ITAM. Expression of DAP12-DN caused considerable cell cycle arrest in G1 and inhibited BrdU incorporation (**Fig. 2e**,**f**). Overall, these data confirm the involvement of DAP12 in M-CSF-driven proliferation.

DAP12 in M-CSF-induced macrophage survival

To assess the function of DAP12 in macrophage survival, we deprived BMDMs of M-CSF for 24 h and measured apoptosis by propidium iodide staining. Wild-type cells were more resistant to apoptosis than were DAP12-deficient BMDMs (**Fig. 3a**,**b**). Retroviral transduction of DAP12 into DAP12-deficient BMDMs resulted in much less apoptosis (**Fig. 3c**), which connected DAP12 deficiency with lower survival.

BMDM cultures contain endogenous M-CSF, which is produced by contaminating fibroblast-like stromal cells. Therefore, to precisely quantify the difference in the M-CSF-induced survival of wild-type and DAP12-deficient BMDMs, we generated pure myeloid precursor cultures free of contaminating fibroblast-like stromal cells[27]. We seeded these precursors for 4 d in equal numbers in various amounts of M-CSF. Pure cultures of wild-type macrophages required exogenous M-CSF for survival, and there was a dose-response relationship between the number of cells that remained after 4 d and the dose of M-CSF (**Fig. 3d**). In contrast, DAP12-deficient cultures had fewer cells than wild-type cultures did at all M-CSF concentrations.

To confirm that DAP12-deficient macrophages die by apoptosis, we cultured BMDMs for 16 h in the presence or absence of M-CSF, then lysed the cells and assessed the presence of active caspase-3 by immunoblot analysis. We detected no active caspase-3 in lysates of wild-type cells grown with or without M-CSF. In contrast, DAP12-deficient cells had large amounts of active caspase-3 after withdrawal of M-CSF (**Fig. 3e**). Together these experiments demonstrate a quantitative defect in M-CSF-induced survival of DAP12-deficient macrophages.

To determine whether wild-type cells produce an extrinsic factor required for the survival of BMDMs, we assessed the survival of wild-type and DAP12-deficient BMDMs cultured together. We mixed bone marrow from DAP12-sufficient, GFP-expressing transgenic mice at a

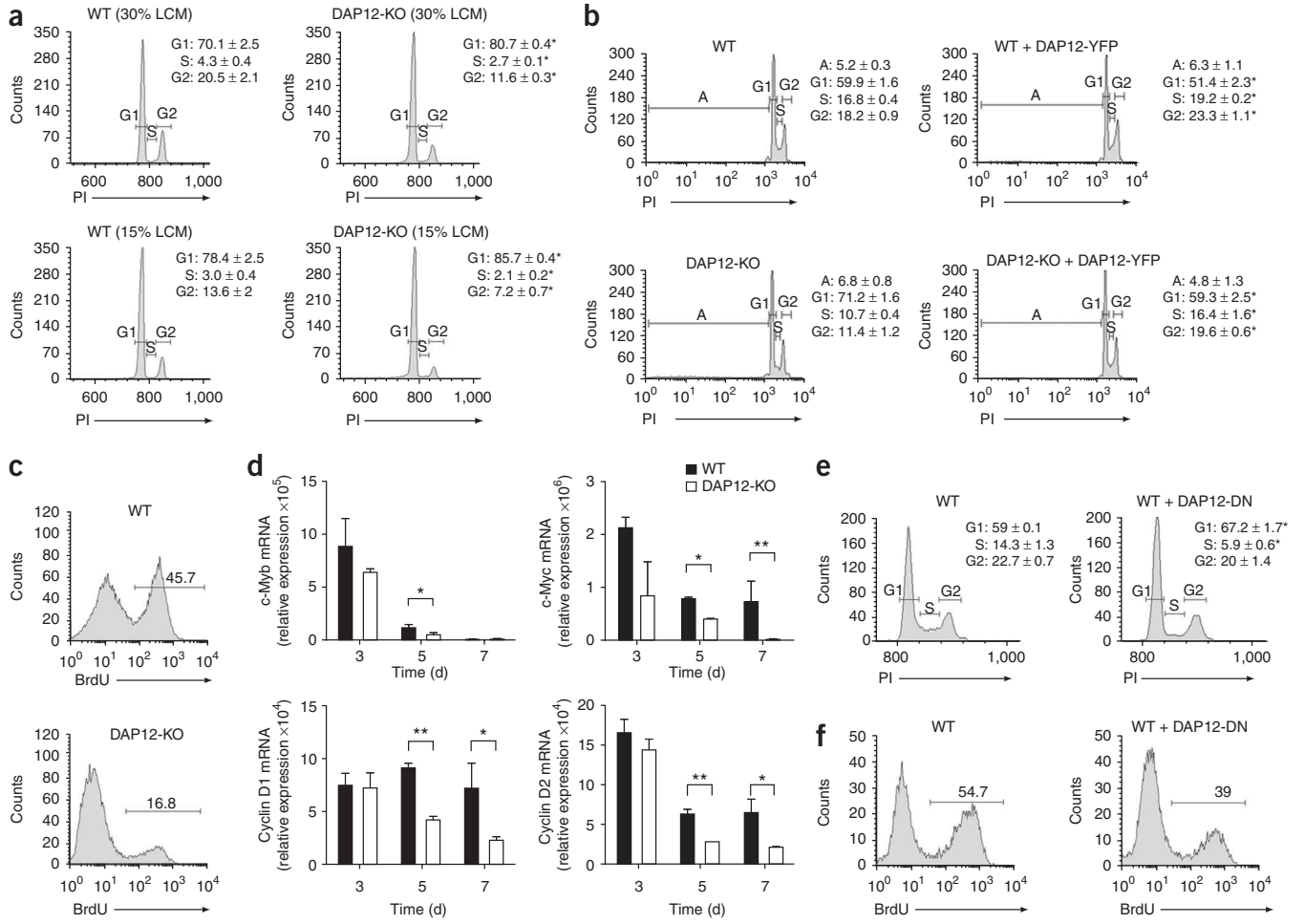

Figure 2 Impaired proliferation of DAP12-deficient BMDMs at day 5 of culture. (**a**) Cell cycle status of wild-type and DAP12-deficient BMDMs, assessed by propidium iodide analysis 24 h after stimulation with 30% or 15% L929 cell–conditioned medium (LCM; mouse connective tissue cells) as a source of M-CSF. Right margin, percentage of total cells in each gate (± s.d.). *, $P < 0.05$ (Student's *t*-test). (**b**) Cell cycle status, assessed as in **a**, of BMDMs transduced with retrovirus encoding DAP12 and yellow fluorescent protein (DAP12-YFP) at day 3 of culture, followed by sorting of YFP^+ and YFP^- cells 2 d later, then replating and culture of cells for 24 h in medium containing 30% LCM. (**c**) Proliferation of wild-type and DAP12-deficient BMDMs at 24 h after incubation with BrdU in the presence of 30% LCM. (**d**) Real-time PCR analysis of the expression of mRNA transcripts in wild-type and DAP12-deficient BMDMs, presented relative to the expression of *Hprt1* (encoding hypoxanthine guanine phosphoribosyl transferase; mean and s.d.). *$P < 0.05$ and **$P < 0.01$ (Student's *t*-test). (**e**,**f**) Propidium iodide analysis of the cell cycle (**e**) and BrdU incorporation analysis of proliferation (**f**) of wild-type BMDMs transduced for 24 h with retrovirus encoding DAP12-DN, followed by treatment as described in **b**. Numbers above bracketed lines (**c**,**f**) indicate percent divided cells. Data are representative of three (**a**,**c**,**d**) or two (**b**,**e**,**f**) experiments.

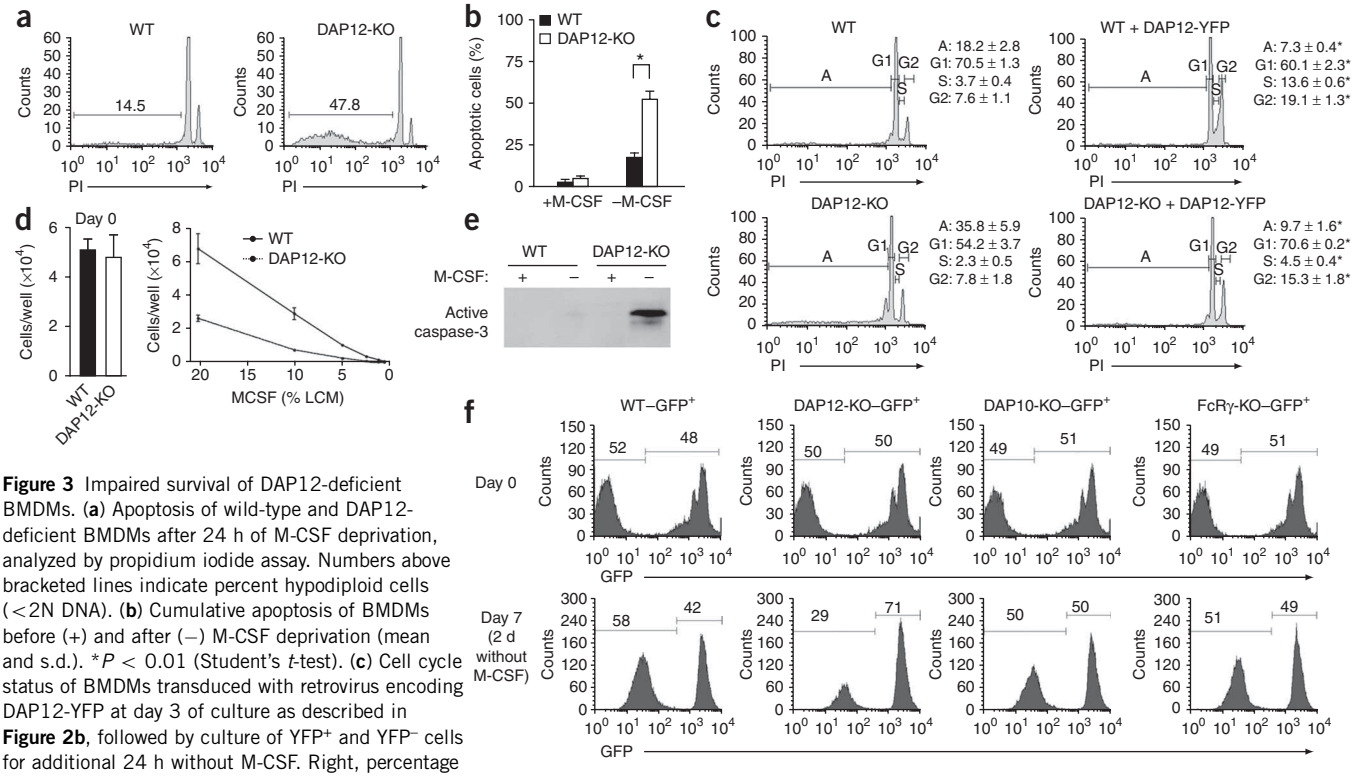

Figure 3 Impaired survival of DAP12-deficient BMDMs. (**a**) Apoptosis of wild-type and DAP12-deficient BMDMs after 24 h of M-CSF deprivation, analyzed by propidium iodide assay. Numbers above bracketed lines indicate percent hypodiploid cells (<2N DNA). (**b**) Cumulative apoptosis of BMDMs before (+) and after (–) M-CSF deprivation (mean and s.d.). $*P < 0.01$ (Student's *t*-test). (**c**) Cell cycle status of BMDMs transduced with retrovirus encoding DAP12-YFP at day 3 of culture as described in **Figure 2b**, followed by culture of YFP⁺ and YFP⁻ cells for additional 24 h without M-CSF. Right, percentage of total cells in each gate (± s.d.). $*P < 0.05$ (Student's *t*-test). (**d**) M-CSF-induced survival of pure cultures of myeloid precursors generated as described before[27], then seeded into 24-well plates at a density of 1×10^5 cells per ml and cultured for 48 h with M-CSF; nonadherent cells were removed and adherent macrophages were counted (left; day 0), then macrophages were cultured for an additional 4 d in LCM as a source of M-CSF (right; concentration, horizontal axis) and cells remaining were counted (mean and s.d.). (**e**) Immunoblot analysis of cleaved (active) caspase-3 in lysates of BMDMs cultured for 16 h in the presence (+) or absence (–) of M-CSF. (**f**) Ratio of GFP⁺ cells to GFP⁻ cells among GFP⁺ and GFP⁻ wild-type, DAP12-deficient, DAP10-deficient or FcRγ-deficient bone marrow cells mixed at a ratio of 1:1 and cultured together for 5 d in the presence of M-CSF, followed by 2 d without M-CSF (Day 7). Numbers above bracketed lines indicate percent GFP⁻ cells (left) or GFP⁺ cells (right). Data are representative of five (**a**,**b**), two (**c**) or three (**d**–**f**) independent experiments.

ratio of 1:1 with bone marrow from wild-type or DAP12-deficient mice and cultured the cells together for 5 d in the presence of M-CSF to generate BMDMs. We continued cultures for 2 additional days in the absence of M-CSF and, on day 7, determined the ratio of GFP⁺ BMDMs to GFP⁻ BMDMs. There was a slight but reproducible predominance of wild-type (GFP⁻) cells over GFP⁺ cells (58% versus 42%) in the cocultures of wild-type and GFP⁺ cells (**Fig. 3f**), which suggested that wild-type cells had a slight survival or proliferation advantage. However, in cocultures of DAP12-deficient cells and GFP⁺ BMDMs, there was selective loss of almost half of the DAP12-deficient (GFP⁻) cells, such that 71% of the cells remaining in culture were GFP⁺.

We did similar studies focusing on the related signaling adaptors DAP10 and FcRγ[17]. However, culture of bone marrow from DAP10-deficient or FcRγ-deficient mice together with GFP⁺ bone marrow suggested that neither DAP10 nor FcRγ influences macrophage proliferation or survival (**Fig. 3f**). These data collectively indicate that the defect in the survival of DAP12-deficient macrophages is specific to DAP12 and, as survival could not be restored by a soluble or cell surface factor present in wild-type cultures, it is cell intrinsic.

Little influence of DAP12 on BMDM differentiation

As macrophage proliferation and differentiation are coordinately regulated[28], we sought to determine whether DAP12 deficiency, although it diminished proliferation, accelerated the differentiation of bone marrow cells into mature macrophages *in vitro*. Both DAP12-deficient and wild-type BMDMs expressed typical macrophage markers, although DAP12-deficient macrophages had lower expression of CD11b, major histocompatibility complex class II, the receptors CD36 and F4/80, and apolipoprotein E, whereas CSF-1R expression was unchanged (**Supplementary Fig. 1** online). Collectively, these observations indicate that lack of DAP12 does not accelerate the M-CSF-induced differentiation of mature macrophages.

Microglial defects in DAP12-deficient mice

Given the considerable defects in the proliferation and survival of DAP12-deficient macrophages in response to M-CSF *in vitro*, we sought to determine whether any abnormality would be manifested *in vivo*. We compared microglia in the brains and spinal cords of wild-type and DAP12-deficient mice by staining for the microglial marker Iba-1 in young mice (4 weeks old) and older mice (10 months old). We found significantly fewer microglia in the basal ganglia (10.6 ± 3.9 cells per mm^2 versus 61.2 ± 8.8 cells per mm^2; $P < 0.001$) and the spinal cord (6.2 ± 4.5 cells per mm^2 versus 37.3 ± 5.8 cells per mm^2; $P < 0.001$; mean ± s.d.) in older DAP12-deficient mice than in wild-type control mice (**Fig. 4**). Furthermore, at high magnification, we found extensive cytoplasmic fragmentation (cytorrhexis) and nuclear condensation characteristic of microglial degeneration and apoptotic cell death in the DAP12-deficient mice (**Fig. 4**). Young wild-type and DAP12-deficient mice had similar numbers of microglia (data not shown). Additionally, we found no detectable differences between wild-type and DAP12-deficient mice in myelopoiesis, circulating myeloid cells or peripheral macrophages in the spleen and liver

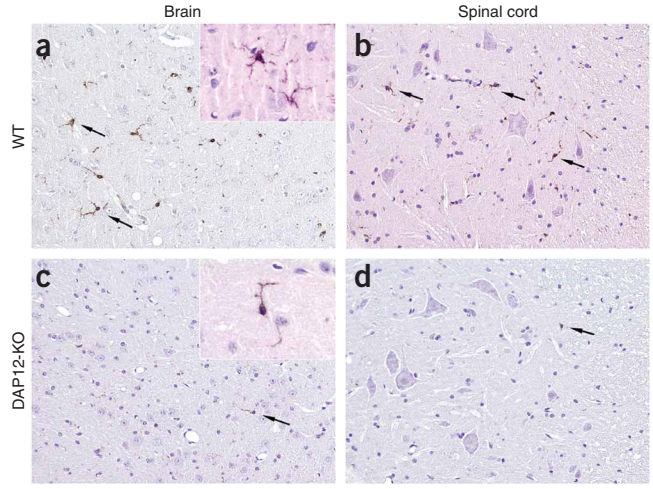

Figure 4 Loss of microglia in CNS of DAP12-deficient mice. Immunohistochemical staining of CNS sections from 10-month-old wild-type mice (**a**,**b**) and DAP12-deficient mice (**c**,**d**) with the microglial marker Iba-1. (**a**,**c**) Basal ganglia brain region. (**b**,**d**) Spinal cord. Arrows indicate microglial cells. Original magnification, ×20 (main images) or ×60 (insets). Data are representative of one experiment with four mice per group.

(**Supplementary Fig. 2** and **Supplementary Table 1** online). On the basis of these observations, we conclude that DAP12 is required for the long-term preservation of a specific microglia subset.

DAP12 in mononuclear phagocyte repopulation

To compare the generation of DAP12-deficient versus wild-type macrophages *in vivo*, we mixed bone marrow from DAP12-sufficient transgenic mice expressing GFP at a ratio of 1:1 with bone marrow from DAP12-deficient (GFP^-) or wild-type (GFP^-) mice (**Fig. 5a**). We then engrafted the mixed bone marrow into lethally irradiated wild-type hosts, which resulted in mice in which the GFP^- bone marrow was either wild-type in origin (wild-type–GFP chimeras) or DAP12-deficient in origin (DAP12-KO–GFP chimeras). We maintained these mice for up to 36 weeks and evaluated bone marrow chimerism by flow cytometry at 12, 19 and 36 weeks after engraftment.

At 12 weeks, the GFP^+ bone marrow/GFP^- bone marrow ratio in the chimeric mice closely reflected the input ratio (**Fig. 5b**). At 19 weeks, the proportion of GFP^+ cells decreased (relative to input) in the wild-type–GFP chimeras, which suggested that the wild-type GFP^- cells were more robust than the GFP^+ cells. In contrast, the proportion of GFP^+ cells remained stable in the DAP12-KO–GFP chimeras, which indicated that the DAP12-deficient cells competed less well than did wild-type cells *in vivo*, much as they did *in vitro*. At 36 weeks, there was a preponderance of GFP^- cells in all chimeras. However, the ratio of GFP^- cells to GFP^+ cells was much greater in the wild-type–GFP chimeras than in the DAP12-KO–GFP chimeras (**Fig. 5b**). There was no deficit in the total number of nucleated cells in the bone marrow (wild-type–GFP and DAP12-KO–GFP chimeras had 2.9×10^7 and 2.6×10^7 nucleated cells per femur, respectively, at 36 weeks, consistent with results obtained with unmanipulated mice (data not shown)). These findings indicate that changes in the GFP^+ cell/GFP^- cell ratio reflected replacement of GFP^+ cells by GFP^- cells. Collectively, these data demonstrate that DAP12-deficient bone marrow cells repopulate the bone marrow of irradiated recipient mice less efficiently than do wild-type cells.

We also assessed peripheral cell populations in the chimeric mice at 36 weeks. We examined blood polymorphonuclear cells ($CD115^-Gr\text{-}1^{hi}$), blood monocytes ($CD115^+Gr\text{-}1^{lo–int}$), peritoneal B cells ($CD19^+$) and peritoneal macrophages ($F4/80^+$; **Fig. 5c**). The GFP^-/GFP^+ ratio of polymorphonuclear cells was about 2:1 in the wild-type–GFP and DAP12-KO–GFP chimeras (**Fig. 5d**). In contrast, the GFP^-/GFP^+ ratio of monocytes in the wild-type–GFP chimeras was greater than that in the DAP12-KO–GFP chimeras (3:1 versus 2:1), similar to that in the bone marrow (**Fig. 5d**). Those findings were consistent with defective proliferation and/or survival of DAP12-deficient monocytes and/or macrophages. In the peritoneum, we found no difference in the GFP^-/GFP^+ ratio of B cells in wild-type–GFP and DAP12-KO–GFP chimeras (about 2:1; **Fig. 5d**). In contrast, there were more peritoneal GFP^- macrophages than GFP^+ macrophages in the wild-type–GFP chimeras (85% versus 15%) than in DAP12-KO–GFP chimeras (75% versus 25%). These results collectively support the idea that DAP12 is involved in promoting the proliferation and survival of monocytes and/or macrophages *in vivo*.

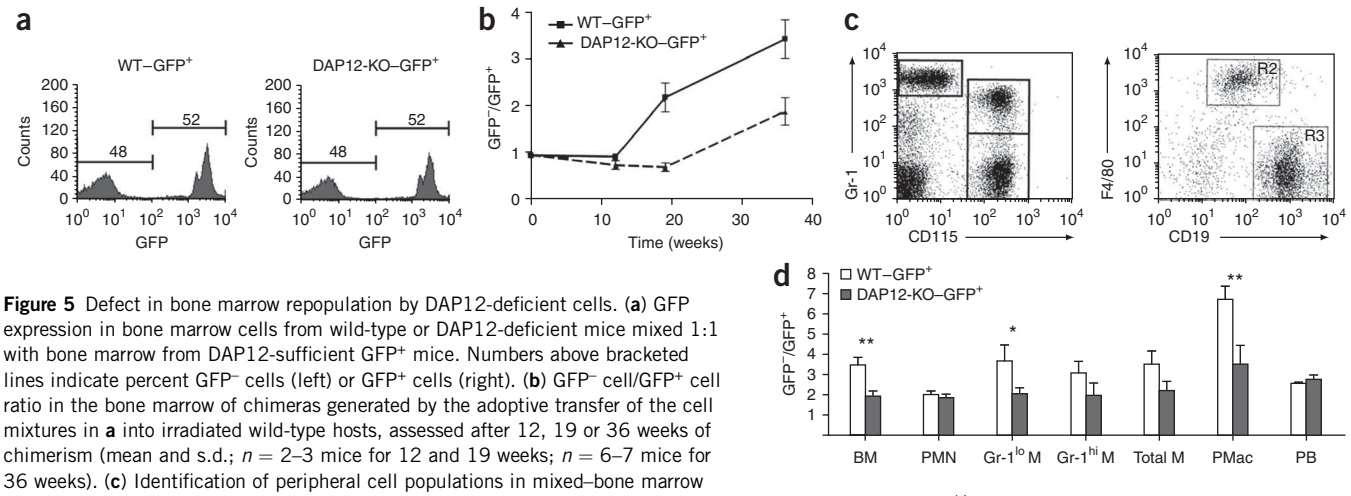

Figure 5 Defect in bone marrow repopulation by DAP12-deficient cells. (**a**) GFP expression in bone marrow cells from wild-type or DAP12-deficient mice mixed 1:1 with bone marrow from DAP12-sufficient GFP^+ mice. Numbers above bracketed lines indicate percent GFP^- cells (left) or GFP^+ cells (right). (**b**) GFP^- cell/GFP^+ cell ratio in the bone marrow of chimeras generated by the adoptive transfer of the cell mixtures in **a** into irradiated wild-type hosts, assessed after 12, 19 or 36 weeks of chimerism (mean and s.d.; $n = 2$–3 mice for 12 and 19 weeks; $n = 6$–7 mice for 36 weeks). (**c**) Identification of peripheral cell populations in mixed–bone marrow (BM) chimeras by surface phenotype (outlined areas): circulating polymorphonuclear cells (PMN), $CD115^-Gr\text{-}1^{hi}$; circulating monocytes (M), $CD115^+Gr\text{-}1^+$; peritoneal B cells (PB), $CD19^+$; peritoneal macrophages (PMac), $F4/80^+$. (**d**) GFP^-/GFP^+ ratio of leukocyte populations from wild-type–GFP and DAP12-KO–GFP chimeras after 36 weeks of chimerism (mean and s.d. of four to seven mice; labels identified above in **c**). $^*P = 0.06$ and $^{**}P < 0.05$ (Student's *t*-test). Data are representative of two separate experiments.

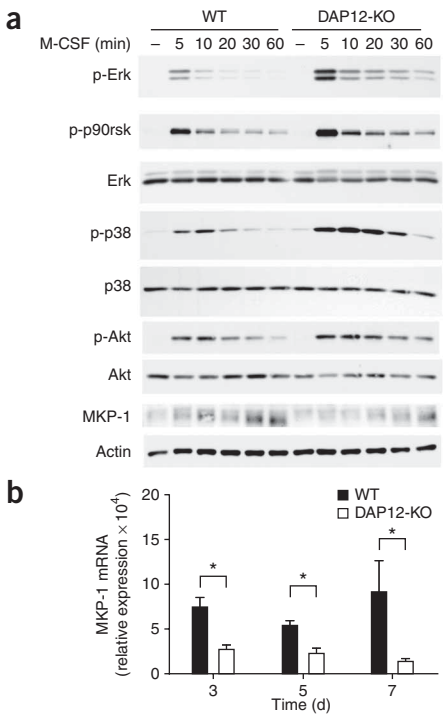

Figure 6 DAP12 deficiency augments M-CSF-induced MAPK activation. (**a**) Immunoblot analysis of phosphorylated (p-) proteins in lysates of BMDMs 'starved' of M-CSF for 4 h and then restimulated with M-CSF (50 ng/ml). Below each blot (and bottom), membranes stripped and reprobed for analysis of the corresponding total protein or actin for normalization of the data. (**b**) Real-time PCR analysis of MKP-1 mRNA transcripts in lysates of BMDMs cultured in M-CSF, presented relative to *Hprt1* expression (mean and s.d.). $*P < 0.01$ (Student's *t*-test). Data are representative of three to five experiments.

DAP12 deficiency skews M-CSF-induced signaling

The inefficient M-CSF-induced proliferation and survival of DAP12-deficient cells indicated that DAP12 is involved in M-CSF signaling. Studies have demonstrated that CSF-1R induces proliferation by activating Erk[29]. Thus, we sought to determine whether CSF-1R requires DAP12 for the activation of Erk and other mitogen-activated protein kinases (MAPKs). We stimulated wild-type and DAP12-deficient BMDMs with M-CSF for various periods of time and analyzed 'downstream' signaling intermediates by immunoblot. M-CSF induced prompt phosphorylation of the MAPKs Erk, p38 and Jnk and the 'downstream' target p90rsk in wild-type cells (**Fig. 6a** and data not shown). DAP12 deficiency did not result in less MAPK activation; in fact, we found slightly but reproducibly greater phosphorylation of Erk, p38 and p90rsk in DAP12-deficient cells (**Fig. 6a**), whereas Jnk phosphorylation was unchanged (data not shown). Thus, the impaired M-CSF-induced proliferation of DAP12-deficient macrophages cannot be accounted for by less activation of Erk.

Notably, it has been reported that M-CSF induces transcriptional activation of MAPK phosphatase 1 (MKP-1)[29], which dephosphorylates p38 and Erk[30]. As DAP12-deficient macrophages were less responsive to M-CSF, we assessed whether they had lower expression of MKP-1 and found that this was indeed the case (**Fig. 6**). This lower MKP-1 expression provides a likely explanation for the paradoxically greater phosphorylation of Erk and p38 in DAP12-deficient cells. Although it has been shown that CSF-1R induces macrophage survival by activating PI(3)K-Akt[29], we found no difference in M-CSF-induced phosphorylation of Akt in DAP12-deficient and wild-type cells (**Fig. 6a**). We conclude that DAP12 controls CSF-1R-induced proliferation and survival through a MAPK-independent pathway.

M-CSF activates β-catenin via DAP12

Among other pathways known to promote cell growth and inhibit apoptosis, the β-catenin pathway was a likely candidate because β-catenin, after nuclear translocation, acts a coactivator of the transcription factors TCF and LEF to induce the transcription of genes involved in the cell cycle (such as those encoding cyclin D1 (refs. 31,32) and c-Myc[33]), which were expressed differently in wild-type and DAP12-deficient BMDMs. Activation of the β-catenin pathway depends on the stabilization of β-catenin and its nuclear translocation[34]. Stability of β-catenin is negatively regulated by GSK3β, which phosphorylates serine and threoinine residues of β-catenin and thereby induces its subsequent proteasome-mediated degradation[34]. Nuclear localization is positively regulated by tyrosine phosphorylation[35,36]. Immunoblot analysis of lysates of BMDMs showed that M-CSF increased the β-catenin in wild-type cells (**Fig. 7a**), which indicates involvement of M-CSF in regulating β-catenin stability. The expression of β-catenin also increased in M-CSF-stimulated DAP12-deficient cells, although to a lesser extent; this finding suggests that DAP12 may influence β-catenin stabilization.

We next sought to determine how M-CSF and DAP12 mediate the activation of β-catenin. M-CSF induced phosphorylation of GSK3β at the serine at position 9 (Ser9) in wild-type BMDMs (**Fig. 7b**). As phosphorylation of Ser9 inhibits GSK3β function, this may explain at least in part the M-CSF-induced stability of β-catenin. Phosphorylation of GSK3β at Ser9 was DAP12 independent, as it was similar in M-CSF-stimulated wild-type and DAP12-deficient BMDMs. M-CSF also induced tyrosine phosphorylation and nuclear translocation of β-catenin in wild-type BMDMs (**Fig. 7c,d**). Notably, M-CSF-induced tyrosine phosphorylation and nuclear translocation of β-catenin were much lower in DAP12-deficient BMDMs (**Fig. 7c,d**). After nuclear translocation, β-catenin activates 'downstream' target genes by interacting with the transcription factors LEF and TCF[34]. To confirm that M-CSF induces the nuclear translocation of β-catenin and activation of LEF and TCF, we transduced wild-type and DAP12-deficient BMDMs with a luciferase reporter driven by three LEF-TCF sites. M-CSF stimulation activated the reporter in wild-type cells but not in DAP12-deficient cells (**Fig. 7e**). Additionally, there was much less nuclear accumulation of β-catenin in wild-type BMDMs transduced with DAP12-DN (**Fig. 7f**). Collectively, these experiments demonstrate that M-CSF activates the β-catenin pathway and that DAP12 is required for M-CSF-induced tyrosine phosphorylation and nuclear translocation of β-catenin.

To confirm the involvement of β-catenin activation in the M-CSF-induced proliferation of BMDMs, we treated wild-type and DAP12-deficient BMDMs with the GSK3β-specific inhibitor SB216763 and measured BMDM proliferation as BrdU incorporation. Inhibition of GSK3β promoted M-CSF-induced the proliferation of BMDMs and restored the proliferation of DAP12-deficient BMDMs to that of wild-type BMDMs (**Fig. 7g**). We conclude that β-catenin activation is crucial for the M-CSF–DAP12 pathway that stimulates BMDM proliferation.

Pyk2 links DAP12 to β-catenin tyrosine phosphorylation

Next we sought to identify molecular mediators that facilitate the DAP12-mediated tyrosine phosphorylation of β-catenin. One plausible candidate was the tyrosine kinase Pyk2. DAP12 activates Pyk2, which results in enhanced signaling of certain cytokines[37,38], and

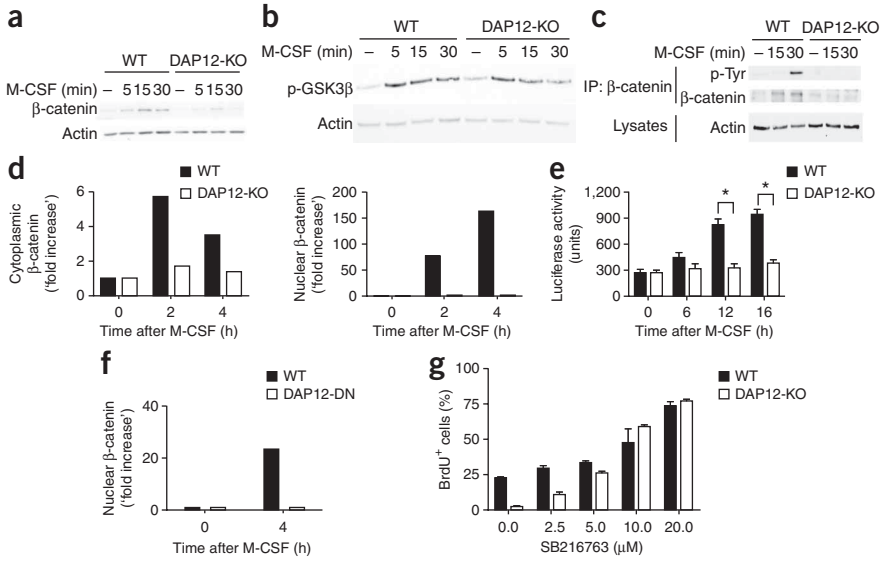

Figure 7 M-CSF activates the β-catenin signaling pathway in a DAP12-dependent way. (**a**) Immunoblot analysis of β-catenin in lysates of BMDMs stimulated for various times (above lanes) with M-CSF (50 ng/ml). (**b**) Immunoblot analysis of GSK3β phosphorylated at Ser9 in lysates of BMDMs stimulated for various times (above lanes) with M-CSF (50 ng/ml). (**c**) Immunoprecipitation (IP) of β-catenin in lysates of BMDMs treated with M-CSF, followed by immunoblot analysis for phosphorylated tyrosine (p-Tyr) and β-catenin. Bottom, immunoblot analysis of actin in total cell lysates before immunoprecipitation (loading control). (**d**) Nuclear translocation of β-catenin in cells treated with M-CSF: lysates were divided into nuclear and cytoplasmic fractions, and β-catenin signals were analyzed by densitometry; results are presented relative to the quantity of glyceraldehyde phosphate dehydrogenase (cytoplasmic fractions) or lamin-B (nuclear fractions). (**e**) Luciferase activity in cells transduced with retrovirus encoding a LEF-TCF–luciferase reporter and stimulated with M-CSF (time, horizontal axis). (**f**) Nuclear translocation of β-catenin in wild-type BMDMs transduced with retrovirus encoding DAP12-DN and stimulated with M-CSF (time, horizontal axis), assessed as described in **d**. (**g**) BrdU incorporation by BMDMs cultured for 8 h in medium containing 30% LCM and BrdU in the presence of various concentrations of the GSK3β inhibitor SB216763, assessed by flow cytometry as percent BrdU$^+$ cells (mean and s.d.). $^*P < 0.05$ (Student's *t*-test). Data are representative of three (**a**–**c**) or two (**d**–**g**) experiments.

Pyk2 mediates the phosphorylation of β-catenin[39]. To directly address whether DAP12 induces the phosphorylation of β-catenin via Pyk2, we stimulated wild-type and DAP12-deficient BMDMs with M-CSF and assessed Pyk2 phosphorylation as a measure of activation. M-CSF induced Pyk2 phosphorylation much more robustly in wild-type BMDMs than in DAP12-deficient BMDMs, and this phosphorylation was inhibited in wild-type BMDMs expressing DAP12-DN (**Fig. 8a**,**b**). Moreover, transduction of wild-type BMDMs with DAP12-DN or a dominant negative form of Pyk2 (CADTK-related non-kinase (CRNK))[40] prevented tyrosine phosphorylation of β-catenin by M-CSF (**Fig. 8c**). Finally, Pyk2 precipitated together with β-catenin from wild-type M-CSF-stimulated BMDMs but not from DAP12-deficient M-CSF-stimulated BMDMs (**Fig. 8d**). To confirm the involvement of Pyk2-mediated β-catenin activation in M-CSF–DAP12–induced proliferation of BMDMs, we showed that two pharmacological inhibitors of Pyk2 inhibited the M-CSF-induced proliferation and cell cycle progression of BMDMs, as assessed by BrdU and propidium iodide assays (**Fig. 8e**). Additionally, transduction of wild-type BMDMs with CRNK resulted in less cell cycle progression and proliferation induced by M-CSF (**Fig. 8f**,**g**).

M-CSF induces activation of the tyrosine kinase Syk through DAP12 in osteoclasts[41]. Therefore, we also evaluated the involvement of Syk in M-CSF-induced β-catenin activation. M-CSF induced DAP12-dependent tyrosine phosphorylation of Syk in BMDMs (**Supplementary Fig. 3a** online), but Syk was not present in β-catenin immunoprecipitates (data not shown), which suggested that Syk has no direct function in DAP12-induced tyrosine phosphorylation of β-catenin. Because a pharmacological inhibitor of Syk inhibited the M-CSF-induced proliferation of BMDMs (**Supplementary Fig. 3b**), it is likely that Syk acts as an 'upstream' activator of the Pyk2–β-catenin pathway.

M-CSF activates β-catenin independently of cell adhesion

It is well established that stimulation of macrophages with M-CSF induces remodeling of the actin cytoskeleton and formation of adhesion structures reflective of integrin activation[42]. Moreover, integrin signaling in macrophages involves DAP12 and Syk[43] and mediates a tonic Pyk2 activation that regulates responsiveness to interferon-α[37]. Thus, M-CSF could trigger the DAP12–Pyk2–β-catenin signaling pathway by promoting 'inside-out' integrin activation. To explore that possibility, we first determined whether DAP12-deficient BMDMs have adhesion defects. In the absence of M-CSF, wild-type and DAP12-deficient BMDMs attached equally well to fibronectin under both static and continuous flow conditions (**Supplementary Fig. 4** online). However, stimulation of BMDMs with M-CSF did not further increase adhesion in these assays, probably because of the considerable basal ability of BMDMs to adhere to fibronectin. Therefore, we investigated M-CSF-induced cytoskeleton reorganization and formation of focal complexes in adherent BMDMs as an indication of macrophage adhesion and integrin activation. After 12 h of M-CSF withdrawal, stimulation of wild-type BMDMs with M-CSF resulted in considerable actin reorganization and cell spreading, with the formation of membrane ruffles, lamellipodia and filopodia (**Supplementary Fig. 5** online). We found nearly identical changes in DAP12-deficient BMDMs. Moreover, staining of wild-type and DAP12-deficient BMDMs with antibody to vinculin (anti-vinculin) showed similar increases in the number and clustering of focal complexes (**Supplementary Fig. 6a** online). M-CSF-induced redistribution of the integrin CD11b was also equivalent in wild-type and DAP12-deficient BMDMs (**Supplementary Fig. 6b**). Thus, M-CSF-induced adhesion and rearrangement of the actin cytoskeleton are not noticeably affected by lack of DAP12, at least in BMDMs.

If the M-CSF–DAP12 pathway to β-catenin activation is independent of integrin signaling, it should occur also when BMDMs are in suspension. M-CSF stimulation of wild-type and DAP12-deficient BMDMs in suspension neither increased their ability to bind a soluble ICAM-1-Fc fusion protein nor enhanced clustering of the integrins VLA-4, CD11b and LFA-1 on the cell surface (data not shown), which indicates that M-CSF does not activate integrins on BMDMs in suspension. However, M-CSF was equally effective in inducing Pyk2 phosphorylation and increasing β-catenin in wild-type BMDMs whether cells were in suspension or attached to plates (**Supplementary Fig. 7** online). These results indicate that

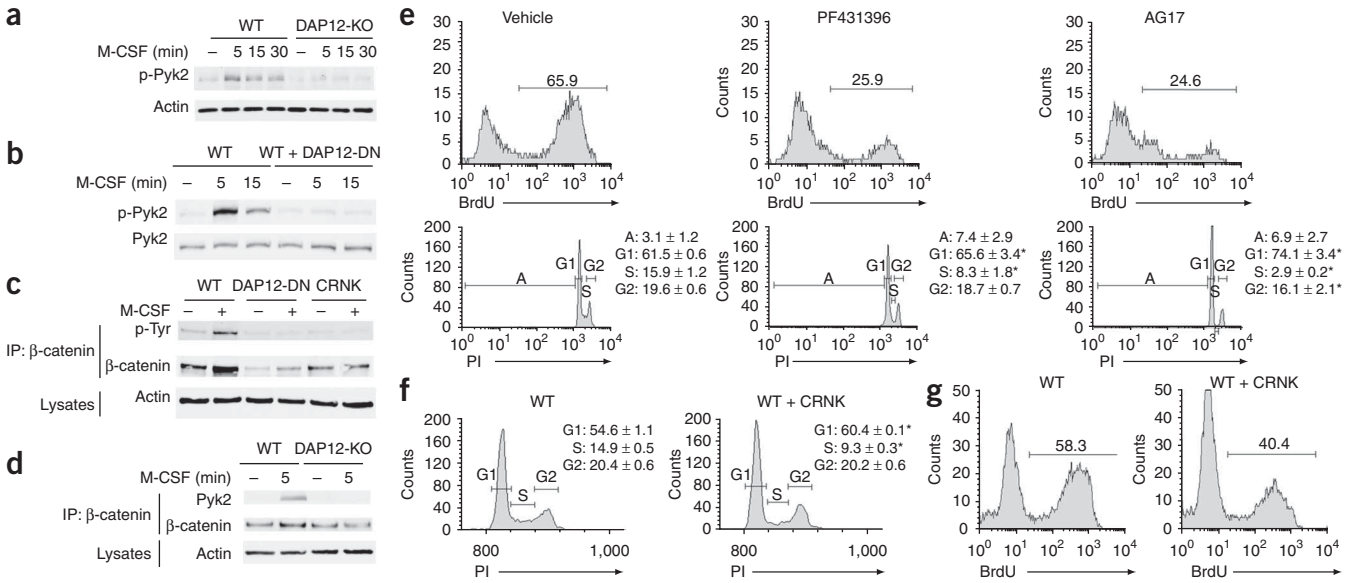

Figure 8 DAP12-mediated tyrosine phosphorylation of β-catenin involves Pyk2. (**a**,**b**) Immunoblot analysis of phosphorylated Pyk2 in lysates of wild-type BMDMs and DAP12-deficient BMDMs (**a**) or wild-type BMDMs transduced with retrovirus encoding DAP12-DN (**b**), stimulated for various times (above lanes) with M-CSF (50 ng/ml). Below, membranes reprobed for actin (**a**) or total Pyk2 (**b**) as a loading control. (**c**) Immunoprecipitation of β-catenin in lysates of wild-type BMDMs transduced with retrovirus encoding DAP12-DN or dominant negative Pyk2 (CRNK), then left untreated (–) or treated for 5 min with M-CSF (+; 50 ng/ml), followed by immunoblot analysis of phosphorylated tyrosine and β-catenin. (**d**) Immunoprecipitation of β-catenin in lysates of BMDMs stimulated for 5 min with M-CSF (50 ng/ml), followed by immunoblot analysis of Pyk2 or β-catenin. Bottom (**c**,**d**), immunoblot analysis of actin in total cell lysates before immunoprecipitation (loading control). (**e**) BrdU incorporation (top) or propidium iodide analysis of the cell cycle (bottom) of wild-type BMDMs cultured for 8 h in medium containing M-CSF (15% LCM) in the presence or absence of the Pyk2 inhibitors PF431396 or AG17 (each at 5 μM). (**f**,**g**) Propidium iodide analysis of the cell cycle (**f**) and BrdU incorporation (**g**) of wild-type BMDMs transduced with retrovirus encoding CRNK and cultured for 24 h in medium containing M-CSF. *$P < 0.05$ (Student's *t*-test). Numbers above bracketed lines (**e**, top; **g**) indicate percent divided cells. Data are representative of three (**a**) or two (**b**–**g**) experiments (**e**,**f**, mean ± s.d.).

the M-CSF activates the DAP12–Pyk2–β-catenin pathway in a cell attachment–independent way.

DISCUSSION

Our report has demonstrated that DAP12 is essential for CSF-1R signaling, specifically for enhancing the proliferation and survival of macrophages in response to M-CSF. Mechanistically, DAP12 facilitated Pyk2-mediated tyrosine phosphorylation and subsequent nuclear translocation of β-catenin. DAP12-deficient macrophages proliferated poorly in response to M-CSF and did not survive in suboptimal amounts of M-CSF *in vitro*. These defects were cell intrinsic. Notably, the impaired responses of DAP12-deficient macrophages to M-CSF *in vitro* had a correlate *in vivo*. Relatively few microglia were present in the basal ganglia and spinal cords of 10-month-old DAP12-deficient mice, and those that remained had an apoptotic phenotype. In addition, DAP12-deficient myeloid precursors reconstituted the monocyte and macrophage compartment less effectively than did precursors from wild-type mice after bone marrow transplantation.

So far, analysis of DAP12-deficient mouse models has yielded ambiguous results regarding the function of DAP12 in microglia[20,22]. Our results have conclusively demonstrated lower numbers and diminished survival of microglia in particular areas of 10-month-old DAP12-deficient CNS; these defects may stem from less responsiveness to M-CSF. Our examination of the basal ganglia and spinal cords of older mice may have made our analysis more sensitive than another published study of this line of DAP12-deficient mice[20].

Notably, mononuclear phagocytes do not uniformly rely on M-CSF for survival[13]. Although osteoclasts and spleen macrophages are entirely M-CSF dependent, microglia require M-CSF only in specific areas of the CNS[14–16]. This may explain why DAP12 deficiency exclusively affected microglia in restricted locations in the CNS. Because microglia are critical for local defense and trophism, confined impairment of microglia in a discrete location may predispose the CNS to distinct pathological defects such as those that occur in NHD. It is possible that DAP12 is involved in M-CSF-induced proliferation and survival of mononuclear phagocytes other than microglia, but a continuous supply of M-CSF may compensate for a lack of DAP12. Future studies should address the contribution DAP12 in conditions in which M-CSF is limiting or rapidly consumed.

In addition to resulting in lower proliferation and survival of mononuclear phagocytes, DAP12 deficiency augmented M-CSF-induced MAPK activation. As M-CSF induces MKP-1 expression[29], impaired responses to M-CSF in DAP12-deficient macrophages may result in lower expression of MKP-1 and consequently more MAPK phosphorylation. Lower MKP-1 expression may also explain the enhanced Erk activation and cytokine responses to Toll-like receptor agonists reported before in DAP12-deficient BMDMs[26].

Notably, we found that CSF-1R activated the β-catenin pathway, which is known to control cell proliferation and survival in other cell types[34]. Activation of the β-catenin pathway depends on stabilization of β-catenin and its nuclear translocation. We found that M-CSF acted on both processes. M-CSF induced phosphorylation of GSK3β at Ser9, which diminished GSK3β kinase activity and therefore promoted β-catenin stability. Additionally, M-CSF induced tyrosine phosphorylation and subsequent nuclear translocation of β-catenin. Although DAP12 had no effect on GSK3β phosphorylation, it was absolutely required for the tyrosine phosphorylation and nuclear accumulation of β-catenin. The diminished nuclear translocation of β-catenin in

DAP12-deficient BMDMs provides a likely explanation for the lower abundance of cyclin D1 and c-Myc mRNA transcripts in these cells than in wild-type BMDMs. Studies have demonstrated that β-catenin is important for the self-renewal and maintenance of hematopoietic stem cells and myeloid progenitor cell pools[44]. Our results have extended those studies, showing that β-catenin is important not only at the stem cell stage but also at later stages of macrophage population expansion and differentiation, when DAP12 and its associated receptors are expressed. This was particularly evident in the mixed–bone marrow chimera experiments, in which DAP12-deficient bone marrow repopulated irradiated hosts but generated fewer mature monocytes and macrophages than did wild-type bone marrow.

Finally, we have identified Pyk2 as the tyrosine kinase that links DAP12 to tyrosine phosphorylation of β-catenin. Published studies have described Pyk2 as a 'downstream' signaling intermediate of DAP12 (refs. 37,38), as well as an effector of β-catenin phosphorylation[39]. Consistent with both observations, we found that M-CSF induced Pyk2 activation and its association with β-catenin in a DAP12-dependent way. The signaling pathway that connects DAP12 and Pyk2 remains to be elucidated. Although M-CSF activates cell adhesion and DAP12 is known to be a mediator of integrin signaling[43], our data indicate that the M-CSF activation of the DAP12–Pyk2–β-catenin pathway is adhesion independent. Thus, this pathway seems to be distinct from the cell attachment–DAP12–Pyk2 pathway that mediates tonic regulation of interferon-α and interleukin 10 signaling[37]. A published study[41] and our own data suggest that M-CSF–DAP12 may act through Syk and possibly other kinases that have been linked to macrophage survival and osteoclast function, such as TEC[45,46]. In conclusion, our identification of a link among M-CSF, the DAP12 ITAM and β-catenin has demonstrated a signaling network that regulates the proliferation and survival of myeloid cells.

METHODS

Methods and any associated references are available in the online version of the paper at http://www.nature.com/natureimmunology/.

Accession codes. UCSD-Nature Signaling Gateway (http://www.signaling-gateway.org): A001489, A000674, A000750, A000506 and A001952.

Note: Supplementary information is available on the Nature Immunology website.

ACKNOWLEDGMENTS

We thank D.M. Ornitz (Washington University School of Medicine) for the LEF-luc-pGL3 reporter plasmid; H.S. Earp III (University of North Carolina, Chapel Hill) for the plasmid encoding CRNK; T. Rolink (University of Basel) for IgM anti-CD4 and IgM anti-CD8; S. Gilfillan for critical reading of the manuscript; C. Laudanna and B. Rossi for advice on cell adhesion experiments; and Pfizer for the Pyk2 inhibitor PF 431396. Supported by the US National Institutes of Health (R01 GM077279 to M.C. and U54 AI1057160 to S.L.S.), Nobel Project Fondazione Cariplo (W.V.) and Fondazione Nocivelli (P.L.P.).

AUTHOR CONTRIBUTIONS

K.O. and I.R.T. designed and did experiments; P.L.P., W.V., T.A. and M.M. did and interpreted immunohistochemistry experiments; E.C., I.T. and A.S.S. did and interpreted adhesion assays and confocal microscopy studies; S.L.S. and T.T. provided reagents and expression data; and M.C. directed the research and wrote the paper.

Published online at http://www.nature.com/natureimmunology/
Reprints and permissions information is available online at http://npg.nature.com/reprintsandpermissions/

1. Stanley, E.R. *et al.* Biology and action of colony-stimulating factor-1. *Mol. Reprod. Dev.* **46**, 4–10 (1997).
2. Chitu, V. & Stanley, E.R. Colony-stimulating factor-1 in immunity and inflammation. *Curr. Opin. Immunol.* **18**, 39–48 (2006).
3. Hamilton, J.A. Colony-stimulating factors in inflammation and autoimmunity. *Nat. Rev. Immunol.* **8**, 533–544 (2008).
4. Sherr, C.J. *et al.* The c-fms proto-oncogene product is related to the receptor for the mononuclear phagocyte growth factor, CSF-1. *Cell* **41**, 665–676 (1985).
5. Downing, J.R., Rettenmier, C.W. & Sherr, C.J. Ligand-induced tyrosine kinase activity of the colony-stimulating factor 1 receptor in a murine macrophage cell line. *Mol. Cell. Biol.* **8**, 1795–1799 (1988).
6. Sengupta, A. *et al.* Identification and subcellular localization of proteins that are rapidly phosphorylated in tyrosine in response to colony-stimulating factor 1. *Proc. Natl. Acad. Sci. USA* **85**, 8062–8066 (1988).
7. Hamilton, J.A. CSF-1 signal transduction. *J. Leukoc. Biol.* **62**, 145–155 (1997).
8. Yeung, Y.G. & Stanley, E.R. Proteomic approaches to the analysis of early events in colony-stimulating factor-1 signal transduction. *Mol. Cell. Proteomics* **2**, 1143–1155 (2003).
9. Tushinski, R.J. & Stanley, E.R. The regulation of mononuclear phagocyte entry into S phase by the colony stimulating factor CSF-1. *J. Cell. Physiol.* **122**, 221–228 (1985).
10. Roussel, M.F. Regulation of cell cycle entry and G1 progression by CSF-1. *Mol. Reprod. Dev.* **46**, 11–18 (1997).
11. Tushinski, R.J. *et al.* Survival of mononuclear phagocytes depends on a lineage-specific growth factor that the differentiated cells selectively destroy. *Cell* **28**, 71–81 (1982).
12. Wiktor-Jedrzejczak, W. *et al.* Total absence of colony-stimulating factor 1 in the macrophage-deficient osteopetrotic (op/op) mouse. *Proc. Natl. Acad. Sci. USA* **87**, 4828–4832 (1990).
13. Cecchini, M.G. *et al.* Role of colony stimulating factor-1 in the establishment and regulation of tissue macrophages during postnatal development of the mouse. *Development* **120**, 1357–1372 (1994).
14. Kondo, Y., Lemere, C.A. & Seabrook, T.J. Osteopetrotic (op/op) mice have reduced microglia, no Aβ deposition, and no changes in dopaminergic neurons. *J. Neuroinflammation* **4**, 31 (2007).
15. Wegiel, J. *et al.* Reduced number and altered morphology of microglial cells in colony stimulating factor-1-deficient osteopetrotic op/op mice. *Brain Res.* **804**, 135–139 (1998).
16. Witmer-Pack, M.D. *et al.* Identification of macrophages and dendritic cells in the osteopetrotic (op/op) mouse. *J. Cell Sci.* **104**, 1021–1029 (1993).
17. Lanier, L.L. DAP10- and DAP12-associated receptors in innate immunity. *Immunol. Rev.* **227**, 150–160 (2009).
18. Paloneva, J. *et al.* Loss-of-function mutations in TYROBP (DAP12) result in a presenile dementia with bone cysts. *Nat. Genet.* **25**, 357–361 (2000).
19. Paloneva, J. *et al.* Mutations in two genes encoding different subunits of a receptor signaling complex result in an identical disease phenotype. *Am. J. Hum. Genet.* **71**, 656–662 (2002).
20. Kaifu, T. *et al.* Osteopetrosis and thalamic hypomyelinosis with synaptic degeneration in DAP12-deficient mice. *J. Clin. Invest.* **111**, 323–332 (2003).
21. Humphrey, M.B. *et al.* The signaling adapter protein DAP12 regulates multinucleation during osteoclast development. *J. Bone Miner. Res.* **19**, 224–234 (2004).
22. Nataf, S. *et al.* Brain and bone damage in KARAP/DAP12 loss-of-function mice correlate with alterations in microglia and osteoclast lineages. *Am. J. Pathol.* **166**, 275–286 (2005).
23. Paloneva, J. *et al.* DAP12/TREM2 deficiency results in impaired osteoclast differentiation and osteoporotic features. *J. Exp. Med.* **198**, 669–675 (2003).
24. Faccio, R., Zou, W., Colaianni, G., Teitelbaum, S.L. & Ross, F.P. High dose M-CSF partially rescues the Dap12−/− osteoclast phenotype. *J. Cell. Biochem.* **90**, 871–883 (2003).
25. Zou, W. *et al.* Syk, c-Src, the $\alpha_v\beta_3$ integrin, and ITAM immunoreceptors, in concert, regulate osteoclastic bone resorption. *J. Cell Biol.* **176**, 877–888 (2007).
26. Hamerman, J.A., Tchao, N.K., Lowell, C.A. & Lanier, L.L. Enhanced Toll-like receptor responses in the absence of signaling adaptor DAP12. *Nat. Immunol.* **6**, 579–586 (2005).
27. Stanley, E.R. Murine bone marrow-derived macrophages. *Methods Mol. Biol.* **75**, 301–304 (1997).
28. Klappacher, G.W. *et al.* An induced Ets repressor complex regulates growth arrest during terminal macrophage differentiation. *Cell* **109**, 169–180 (2002).
29. Xaus, J. *et al.* Molecular mechanisms involved in macrophage survival, proliferation, activation or apoptosis. *Immunobiology* **204**, 543–550 (2001).
30. Owens, D.M. & Keyse, S.M. Differential regulation of MAP kinase signalling by dual-specificity protein phosphatases. *Oncogene* **26**, 3203–3213 (2007).
31. Tetsu, O. & McCormick, F. Beta-catenin regulates expression of cyclin D1 in colon carcinoma cells. *Nature* **398**, 422–426 (1999).
32. Shtutman, M. *et al.* The cyclin D1 gene is a target of the β-catenin/LEF-1 pathway. *Proc. Natl. Acad. Sci. USA* **96**, 5522–5527 (1999).
33. He, T.C. *et al.* Identification of c-MYC as a target of the APC pathway. *Science* **281**, 1509–1512 (1998).
34. Clevers, H. Wnt/β-catenin signaling in development and disease. *Cell* **127**, 469–480 (2006).
35. Lilien, J. & Balsamo, J. The regulation of cadherin-mediated adhesion by tyrosine phosphorylation/dephosphorylation of β-catenin. *Curr. Opin. Cell Biol.* **17**, 459–465 (2005).
36. Piedra, J. *et al.* Regulation of β-catenin structure and activity by tyrosine phosphorylation. *J. Biol. Chem.* **276**, 20436–20443 (2001).
37. Wang, L. *et al.* 'Tuning' of type I interferon-induced Jak-STAT1 signaling by calcium-dependent kinases in macrophages. *Nat. Immunol.* **9**, 186–193 (2008).

38. Hu, X., Chen, J., Wang, L. & Ivashkiv, L.B. Crosstalk among Jak-STAT, Toll-like receptor, and ITAM-dependent pathways in macrophage activation. *J. Leukoc. Biol.* **82**, 237–243 (2007).
39. van Buul, J.D., Anthony, E.C., Fernandez-Borja, M., Burridge, K. & Hordijk, P.L. Proline-rich tyrosine kinase 2 (Pyk2) mediates vascular endothelial-cadherin-based cell-cell adhesion by regulating β-catenin tyrosine phosphorylation. *J. Biol. Chem.* **280**, 21129–21136 (2005).
40. Li, X., Dy, R.C., Cance, W.G., Graves, L.M. & Earp, H.S. Interactions between two cytoskeleton-associated tyrosine kinases: calcium-dependent tyrosine kinase and focal adhesion tyrosine kinase. *J. Biol. Chem.* **274**, 8917–8924 (1999).
41. Zou, W., Reeve, J.L., Liu, Y., Teitelbaum, S.L. & Ross, F.P. DAP12 couples c-Fms activation to the osteoclast cytoskeleton by recruitment of Syk. *Mol. Cell* **31**, 422–431 (2008).
42. Pixley, F.J. & Stanley, E.R. CSF-1 regulation of the wandering macrophage: complexity in action. *Trends Cell Biol.* **14**, 628–638 (2004).
43. Mocsai, A. *et al.* Integrin signaling in neutrophils and macrophages uses adaptors containing immunoreceptor tyrosine-based activation motifs. *Nat. Immunol.* **7**, 1326–1333 (2006).
44. Scheller, M. *et al.* Hematopoietic stem cell and multilineage defects generated by constitutive β-catenin activation. *Nat. Immunol.* **7**, 1037–1047 (2006).
45. Melcher, M. *et al.* Essential roles for the Tec family kinases Tec and Btk in M-CSF receptor signaling pathways that regulate macrophage survival. *J. Immunol.* **180**, 8048–8056 (2008).
46. Shinohara, M. *et al.* Tyrosine kinases Btk and Tec regulate osteoclast differentiation by linking RANK and ITAM signals. *Cell* **132**, 794–806 (2008).

ONLINE METHODS

Mice. All animal studies were approved by the Washington University Animal Studies Committee. B6.129P2-TYROBPtm1Ttk mice (called 'DAP12-deficient mice' here) and B6.129P2-HCSTtm1cln mice (called 'DAP10-deficient mice' here) have been described[20,47]. C57BL/6-Tg(UBC-GFP)30Scha/J mice (called 'GFP$^+$ mice' here) were from Jackson Laboratories. B6.129P2-Fcεr1gtm1Rav mice (called 'FcRγ-deficient mice' here) and wild-type control C57BL/6 mice were from Taconic Laboratories.

DNA constructs. An LEF-luc-pGL3 reporter plasmid was provided by D.M. Ornitz. An *Xho*I-*Sal*I DNA fragment including three LEF sites, the *Fos* promoter and the luciferase gene was subcloned into the *Xho*I site of the retroviral vector pMX[48] in the 3′-5′ orientation relative to the pMX promoter. A plasmid encoding CRNK, which corresponds to the C-terminal noncatalytic domain of Pyk2, was provided by H.S. Earp III. A DNA fragment encompassing CRNK was subcloned into pMX-IRES-GFP[48]. A YFP-tagged DAP12 molecule was constructed and cloned into the pMX retrovirus vector[49]. DAP12-DN was generated from YFP-tagged DAP12 by mutation of the sequence encoding ITAM tyrosine residues into sequence encoding phenylalanine residues as described[50].

Generation and transduction of BMDMs. BMDMs were differentiated *in vitro* from bone marrow cells cultured in BMDM differentiation medium containing 30% LCM as a source of M-CSF. At day 5 (or at other times where stated otherwise), nonadherent cells were removed and adherent cells were used. For BMDM transduction, retroviral constructs were transiently transfected into Plat-E packaging cells with FuGENE 6 transfection reagent (Roche). Virus was collected after 2 d and was exposed to BMDMs at day 3 of culture for 24 h in the presence of polybrene (4 μg/ml; Sigma). Cells were further cultured in BMDM differentiation media for 1 additional day. At this point, both YFP$^+$ (or GFP$^+$) and YFP$^-$ (or GFP$^-$) cells were sorted by flow cytometry, cultured overnight in BMDM differentiation media and then used for experiments. Where indicated, BMDMs were derived from a pure population of myeloid precursors, generated as described[27].

Analysis of cell cycle and apoptosis. Cell cycle and cell death status were determined on the basis of the DNA content of cells. Cells were washed with flow cytometry buffer (2% (vol/vol) FCS in PBS), fixed with 70% ethanol and stained with propidium iodide according to established protocols. Samples were analyzed on a FACStar (BD Biosciences).

Proliferation assay. M-CSF-stimulated cells were labeled for 8 or 20 h with BrdU (5-bromodeoxyuridine; 50 μg/ml) and incorporation was measured by flow cytometry with a FITC BrdU Flow kit (BD Pharmingen). In some experiments, proliferation and cell cycle analysis were done in the presence of the Pyk2 inhibitors PF431396 (provided by Pfizer) and AG17 (Calbiochem) or a Syk inhibitor (Calbiochem).

RNA isolation and quantitative PCR. At various times during culture, total RNA was extracted from BMDMs with TRIzol reagent according to the manufacturer's instructions (Invitrogen). After first-strand cDNA synthesis with a SuperScript first-strand synthesis system for RT-PCR (Invitrogen), real-time quantitative PCR was done on a Bio-Rad iCycler. Reactions were set up with an iQ SYBR Green Supermix (Bio-Rad) and specific primers (**Supplementary Table 2** online). For relative quantification, target mRNA expression was calculated, normalized to the expression of *Hprt1*, and is presented as (target gene mRNA / *Hprt1* mRNA).

CNS histology. Wild-type and DAP12-deficient mice were killed at 10 months after birth. Brains and spinal cords were removed and were fixed overnight in 4% (wt/vol) paraformaldehyde. Tissue samples were embedded in paraffin, and sections 4 μm in thickness were cut and stained for histological examination. Routine hematoxylin and eosin staining was used for the study of basic histopathological changes. Immunohistochemistry was used to investigate microglial morphology and distribution. Sections were dewaxed and rehydrated and endogenous peroxidase activity was blocked for 15 min with 0.3% (vol/vol) H_2O_2 in methanol. Microwave treatment in 1.0 mM EDTA buffer, pH 8.0, was used for epitope retrieval. Sections were then washed, preincubated for 5 min in blocking buffer containing 5% (vol/vol) normal goat serum in Tris-HCl and incubated for 2 h with polyclonal rabbit primary antibody to Iba-1 (1:500 dilution; 019-19741; Wako-Chem) in Tris and 1% (wt/vol) BSA. Sections were then washed in Tris-HCl buffer before being incubated for 30 min with secondary antibody (ChemMATE Envision Rabbit/Mouse; DAKO Cytomation). Signals were visualized with diaminobenzydine and slides were counterstained with hematoxylin. Images were obtained with an Olympus DP70 camera mounted on an Olympus Bx60 microscope with Cell-F imaging software (Soft Imaging System). Five different representative spinal cord and brain sections for each mouse counting were used for quantification; for this, Iba-1$^+$ cells present in each area were counted.

Immunoprecipitation and immunoblot. BMDMs were cultured for 4 h in medium without LCM and then were collected and replated onto non–tissue culture plates. Cells were stimulated with mouse M-CSF (R&D Systems) for the appropriate time and were lysed in buffer containing 1% (vol/vol) Nonidet-P40 and inhibitors as described[49]. For immunoprecipitation of β-catenin, 200 μg cell lysate was immunoprecipitated with anti-β-catenin (9562; Cell Signaling Technology) and protein A Sepharose (GE Healthcare). Cell lysates were separated by standard SDS-PAGE and analyzed by immunoblot. Antibodies to the following were used: active caspase 3 (9661), phosphorylated Erk (9101), phosphorylated p90RSK (9344), p38 (9212), phosphorylated p38 (9211), Akt (9272), phosphorylated Akt (9271), GSK3β phosphorylated at Ser9 (9336), Jnk (9252), phosphorylated Jnk (9251), Syk (2712), β-catenin (9562) and glyceraldehyde phosphate dehydrogenase (14C10; all from Cell Signaling Technology); phosphorylated tyrosine (4G10, Upstate); Erk2 (C-14), β-actin (C-11), Syk (N-19), MKP-1 (V-15) and lamin B (C-20; all from Santa Cruz Biotechnology); and Pyk2 (610548; BD Transduction Labs) and phosphorylated Pyk2 (44-632; BioSource).

Bone marrow chimeras. Recipient mice were irradiated with γ-irradiation (950 rads) for ablation of endogenous bone marrow. Donor bone marrow was isolated from the femurs and tibia of mice and red blood cells were lysed with RBC lysis buffer (Sigma). CD4$^+$ and CD8$^+$ T cells were eliminated by incubation for 20 min at 37 °C with IgM anti-CD4 (RL172) and IgM anti-CD8 (31M; both from T. Rolink) in PBS plus 5% (wt/vol) BSA, followed by the addition of 1 ml rabbit complement (Cedar Lane) and incubation for an additional 45 min at 37 °C. Cells were washed twice with PBS plus 5% (wt/vol) BSA and resuspended in DMEM and 1×10^7 cells were transferred intravenously into each host mouse.

Additional methods. Information on adhesion assays and immunofluorescence is available in the **Supplementary Methods** online.

47. Gilfillan, S., Ho, E.L., Cella, M., Yokoyama, W.M. & Colonna, M. NKG2D recruits two distinct adapters to trigger NK cell activation and costimulation. *Nat. Immunol.* **3**, 1150–1155 (2002).
48. Kitamura, T. *et al.* Retrovirus-mediated gene transfer and expression cloning: powerful tools in functional genomics. *Exp. Hematol.* **31**, 1007–1014 (2003).
49. Giurisato, E. *et al.* Phosphatidylinositol 3-kinase activation is required to form the NKG2D immunological synapse. *Mol. Cell. Biol.* **27**, 8583–8599 (2007).
50. Chen, X. *et al.* A critical role for DAP10 and DAP12 in CD8$^+$ T cell-mediated tissue damage in large granular lymphocyte leukemia. *Blood* **113**, 3226–3234 (2009).

doi:10.1038/ni.1744